Bulletin of the JSME, Vol. 17, No. 113, November, 1974

539.43.013.1

Heat Generation Associated with Rotating Bending Fatigue of a Steel and Deduction of the Fatigue Notch Factor*

By Masakazu HIGUCHI,**
Yasufumi IMAI*** and Minoru TAKENAKA****

. Noncontact measurement was made of the surface temperatures of steel specimens subjected to rotating bending. The temperature variation was expressed as the sum of two exponential functions with due consideration for heat transmission. The thermal energy produced during one stress cycle could be regarded to be almost constant throughout the main fatigue process and its stress dependence was found to be expressible in an exponential function of the reciprocals of the stress amplitudes. A fatigue criterion has been obtained, which agrees with the results presented by others from the standpoint of hysteresis energy dissipation, and, being applied to the notched specimens, gives a means to determine the fatigue notch factors. The calculated values have been shown to agree satisfactorily with the data in the literature.

1. Introduction

When Ono[1] estimated the thermal dissipation during fatigue tests, his concern was in the difference in the free energies of his specimens before and after fatigue, which was regarded as alloted to fatigue the material. In contrary to his and other viewpoints of the same kind[2], we suppose that, although the mechanical energy supplied by the repeating load is in the main lost as heat, the thermal energy would not be a wasteful part unrelated to the work for fatiguing the material, but be a kind of frictional heat closely associated with the quantity of the microscopic plastic flows which lead to fatigue damage; it would be a track, so to speak in terms of energy, of the process of fatigue damage accumulation; such heat would give a clue correlating the fatigue damage accumulation to the movements, multiplications and mutual interactions of dislocations.

However, the way to consider the process in an integrated form now seems to have been rejected, and importance has come to be attached to observing the microcracks themselves and analyzing their micromechanical behavior probably since those days, when Wadsworth[3] noticed that changes in surface conditions could affect crack formation without altering the bulk energy dissipation, so a direct connection between energy loss and fatigue was recognizable only under the same conditions.

Accordingly, under the same conditions of the specimens, we assume that cracking is initiated when the accumulation of the microscopic plastic flows, that is, the generated heat accumulation attains a certain critical amount, and we formulate a criterion for macrocrack initiation.

This is applied to the notch bottom region of a notched specimen and a formula is deduced for evaluation of the fatigue notch factor.

2. Heat generation associated with fatigue of a carbon steel S50C

2.1 Specimens

Specimens were taken from rolled circular rods of 22 mm in diameter and 5.5 m in length. After being annealed at 833 C for 1 hour, they were lathed to a form as illustrated in Fig. 1; thereafter they were annealed at 600 C for 1 hour again and their test surfaces were electropolished about 20 μm.

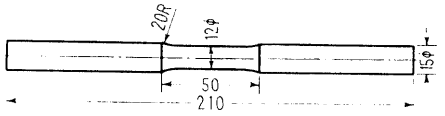

Fig. 1 Rotating bending fatigue specimen Sizes are in mm.

A rotary bending testing machine of Ono-type was used. Chemical composition and mechanical properties of the annealed material are shown in Table 1.

2.2 Testing procedure

Noncontact measurement of the surface temperature during the fatigue process was made using an infra-red microscope (Barnes

* Received 20th November, 1972.
** Professor, Research Institute for Applied Mechanics, Kyushu University, Fukuoka.
*** Lecturer, Faculty of Engineering, Nagasaki University, Nagasaki.
**** Technical Official, Research Institute for Applied Mechanics, Kyushu University, Fukuoka.

Table 1 Chemical composition and mechanical properties

Material	Chemical composition %							
	C	Si	Mn	P	S	Cu	Al	Ni+Cr
S50C	0.54	0.28	0.77	0.017	0.016	0.06	0.017	0.07

Mechanical properties kg/mm^2, %			
Lower yield point	Tensile strength	Fracture stress	Reduction of area
35.4	68.7	105.2	42.3

RM-2A, sensitivity 0.5 deg. at room temperature, resolution 0.5 mm and response time 8 μsec). The emissivity of the specimen surface as polished had been found below 0.2. A recommended paint of high emissivity (3M velvet coating, 101-C10 black) was sprayed on the specimen, circumferentially in the middle part. For the temperature calibration, calibration sources (RM-121, RM-122) were used together with a temperature controller (RM-122-2).

2.3 Formulation of the measured temperatures as a function of N

Typical examples of the records of the temperature changes are shown in Figs. 2 and 3, their ordinates being in units of heat energy and degree in centigrades, respectively. The temperature variations are, as shown in Fig. 3, expressible by the following formula except those in the final stage just before the break of the specimen.

$$\theta = C_o(1 - e^{-m\lambda N}) + D_o(1 - e^{-n\lambda N}) \quad (1)$$

where θ is the temperature variation of the specimen surface from the ambient temperature in centigrades, N the number of stress cycles, λ the time required for one stress cycle in seconds, and C_o, D_o, m and n are constants. It was reported in previous papers[4]-[6] that for polymers, unlike the metal, one term of the right-hand side of Eq. 1 sufficed to formulate the temperature variation. This dissimilarity is supposed due in the main to the difference of their thermal diffusibilities. Because of good heat conductivity in metals, some parts of the testing machine, especially the grips, would also have been heated up by conduction from a specimen during the fatigue test. As a result, their temperature variations could not be neglected. This may be shown as follows.

We now assume two virtual bodies at a homogeneous effective temperature θ_e above the ambient when the specimen is at θ, each adjoining each of the specimen ends. Their incremental changes are expressed (linearity being assumed valid) as

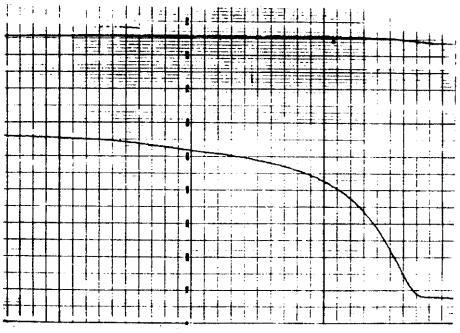

Fig. 2 One of records of specimen surface temperature changes due to fatigue heat generation
The ordinate is in the unit of radiation energy. It begins at the right.

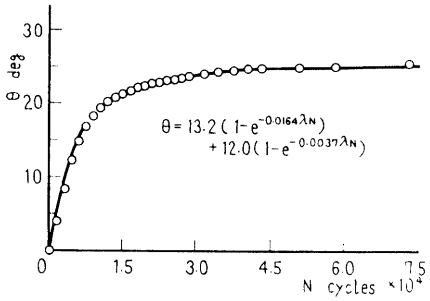

Fig. 3 Temperature variation of a steel specimen as represented by Eq. (1).
Open circles are for measured points on the record in Fig. 2 and the line illustrates the equation written.

$$d\theta = H \cdot dN - h_1 \cdot \theta \cdot dt - h_2(\theta - \theta_e) \cdot dt$$

$$d\theta_e = h_3 \cdot (\theta - \theta_e) \cdot dt - h_4 \cdot \theta_e \cdot dt$$

where H is the heat generation rate (deg cycle^{-1}) which represents the thermal energy produced during one stress cycle per unit volume when multiplied by the specific heat and the density of the specimen material, and h_1, h_2, h_3 and h_4 are constants

(sec^{-1}), which are characteristics of thermal diffusion. In the case of an N-independent H, the same expression as Eq. (1)

$$\theta = \frac{H(m - h_3 - h_4)}{m(m - n)\lambda}(1 - e^{-m\lambda N}) + \frac{H(n - h_3 - h_4)}{n(n - m)\lambda}(1 - e^{-n\lambda N}) \qquad (2)$$

is obtained from the above differential equations.

Other conceivable reason for the different mode of temperature variation from plastics would be such that the H for the metal may vary with N unlike those polymers previously investigated. We recorded cooling curves of the specimens rotating under no load when they were released from the loads after their temperatures had attained their ceiling values (see Fig. 4). The cooling curves involve no heat generation and, as a matter of course, are not affected by the change in H. Those curves also fitted Eq. (1) with the same characteristic constants and with $H = 0$ as well. Therefore the above derivation of Eq. (1) was considered appropriate.

No thought was given to the rapid increase of the specimen temperature just before the break, during which localized large scale plastic flows occurred owing to the propagation of macrocracks; this period, which is called the stage III[7], was rather short; at the beginning of this stage the strength of the material, we can say, had run out in effect.

2.4 Heat generation rate and thereby defined fatigue criterion

Comparing Eq. (1) with Eq. (2), we get the relation

$$H = (C_0 m + D_0 n) \lambda \qquad (3)$$

In order to evaluate H, we take an appropriate value of N and putting θ_1, θ_2 and θ_3 as the temperatures above the surroundings at N, $2N$ and $3N$ cycles, respectively, we obtain

$$\begin{Bmatrix} m \\ n \end{Bmatrix} = -\frac{1}{\lambda N}\ln\{\begin{matrix} p \\ q \end{matrix}$$

$$C_0 = (q\theta_\infty - S_1)/(q - p)$$

$$D_0 = (p\theta_\infty - S_1)/(p - q)$$

Here $S_i = \theta_\infty - \theta_i$ (i=1,2,3) and θ_∞ is the steady state temperature; p and q are obtained by solving the equations

$$q = \frac{S_2 \cdot p - S_3}{S_1 \cdot p - S_2} = \frac{S_1 \cdot p - S_2}{\theta_\infty \cdot p - S_1}$$

Thus-obtained heat generation rates have been found to be related to the respective fatigue lives N_f as

$$(H - a) \cdot N_f = 2.6 \times 10^3 \quad (\mathrm{deg}) \qquad (4)$$

$$a = 0.003 \quad (\mathrm{deg/cycle})$$

which is illustrated in Fig. 5. A similar relation was previously obtained for some polymers too[4]-[6].

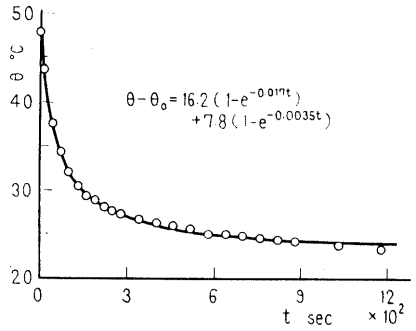

Fig. 4 An example of temperature decrease measured after the test was interrupted

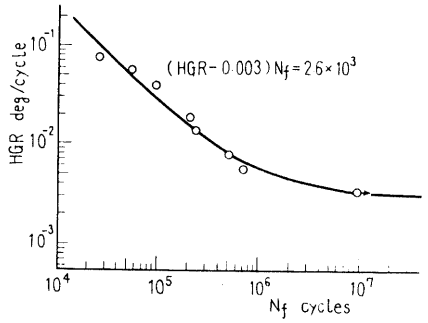

Fig. 5 Relation between heat generation rate H and fatigue life N_f

2.5 Stress amplitude dependence of H

The values of H/σ_a plotted on a semi-log scale against the reciprocals of the stress amplitudes σ_a lie nearly on a straight line as seen in Fig. 6. That is, the heat generation rate is expressible by

$$H = C_1 \cdot \sigma_a \cdot \exp(-\sigma^*/\sigma_a) \qquad (5)$$

The exponential factor* in the formula is regarded as expressing the mean velocity of the dislocations in crystals under stress[8].

In a limited range of the stress amplitude, however, the formula can be approxi-

* As will be described later, the factor rapidly decreased with σ_a. Therefore the expression itself has been used for simplicity in place of its integral over the range of fluctuation of the stress.

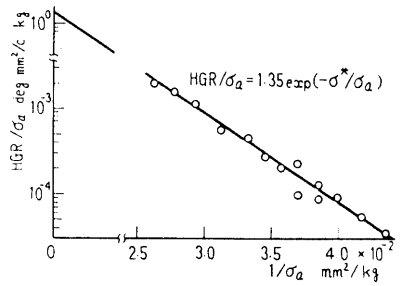

Fig. 6 Relation between heat generation rate and applied stress amplitude σ_a
The straight line illustrates the equation written with $\sigma^* = 245$ kg/mm^2.

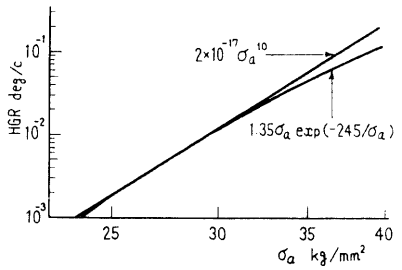

Fig. 7 Comparison of relations expressed by Eq. (5) and Eq. (6)

mated by

$$H = C_2 \cdot \sigma_a^{\,n} \qquad (6)$$

and the exponent $n = 10$ has been obtained for our material. This approximate formula is well compared with the above exact one as seen in Fig. 7. We will use the expression (6) for simplicity in the following treatment.

The rotary bending stresses are not uniform across the section of the specimen. Consequently, our case is to measure the H in the whole section on the average and to relate it only for convenience' sake to the maximum bending stress in the specimen. We now presume that the thermal energy generated in any part of the specimen is similarly expressible by Eq. (6), depending on the stress which the part undergoes. Then the average of the H of the disk-shaped section of the radius R and the thickness t, being subject to reversed bending stresses of the amplitude σ_a on the periphery, is

$$H = 4C_4/(\pi R^2 t)\int_0^{\pi/2}\int_0^{R}(\sigma_a r/R)^n \, tr \, dr \, d\phi$$

$$= C_3\sigma_a^{\,n} \qquad (7)$$

This is again related to the maximum of the bending stresses. It differs from Eq. (6) only in the value of the coefficient*. This is consistent with our presupposition.

3. Deduction of the fatigue notch factor

To employ such a criterion of fatigue as is given by Eq. (4) is to admit the existence of an endurance limit. N_f tends to infinity in the case H is small enough to be nearly equal to a. The stress amplitude in this limiting case is given by Eq. (5) with $H = a$. If the applicability of the same criterion to the notched specimen is assumed, then the fatigue notch factor is derived as follows.

3.1 Heat generation rate in the notched section

Suppose a circumferentially grooved circular rod undergoing rotary bending. The bending stress distribution can be expressed as

$$\sigma = \sigma_a \cdot f(r) \cdot \cos w \qquad (8)$$

at a radius r and an angular coordinate w on the notched section. Here σ_a is the nominal stress at the notch bottom, and $f(r)$ is a function of r, dependent on the notch geometry. The fatigue limit of a notched specimen, σ_a, is defined by σ_w/β, where σ_w is the fatigue strength of the plain specimen and β is the notch factor. Therefore

$$H_{\text{notched}} = C_4\int_{R-\delta}^{R}\left\{\frac{\sigma_w}{\beta} f(r)\right\}^n r\,dr \qquad (9)$$

The non-zero lower limit of integration is taken with regard to the fact that the fatigue damage concentrates within a region of the depth δ inward from the surface[9]. For an unnotched specimen undergoing reversed bending stress of the same amplitude,

$$H_{\text{unnotched}} = C_4\sigma_w^{\,n}R^2/\{(n+2)K^n\} \qquad (10)$$

where

$$K = \{1 - (1 - \delta/R)^{n+2}\}^{-1/n} \qquad (11)$$

We assume the identical criterion for the H and equate the right-hand sides of Eq. (9) and Eq. (10) with each other. We get

$$\beta = K\left[(n+2)/R^2\int_{R-\delta}^{R}\{f(r)\}^n r\,dr\right]^{1/n} \qquad (12)$$

which comes out σ_a-independent, as is naturally expected.

---

* We once calculated the temperature distribution across the section of a plate specimen subjected to plain bending. The distribution was found very even; about a few percent lower on the surface as well as in the center than the average.

By way of example we take a deep hyperbolic notch, the stress distribution for which is given by Neuber[10],

$$\sigma = \sigma_a \frac{\tan v}{\tan v_0}\left(A + B \frac{\cos^2 v_0}{\cos^2 v}\right)\cos w \quad (13)$$

where

$$r/R = \sin v/\sin v_0, \quad \sin v_0 = \sqrt{R}/\sqrt{R+\rho}$$
$$A = 3/(4N)\cdot(1 + \sqrt{1+R/\rho})\{3R/(2\rho) - (1-2\nu)\sqrt{1+R/\rho} + 5/2 + \nu\}$$
$$B = 9/(8N)\cdot(1 + \sqrt{1+R/\rho})\cdot(1 + R/\rho)$$
$$N = \sqrt{1+R/\rho}\ \{1 + 4\nu + (1+\nu)\rho/R\} + 3(1+R/\rho) - (1+\nu)\rho/R$$

R being the radius of the minimum section and ρ the notch radius. Therefrom the fatigue notch factor is calculated.

$$\beta = K\left[(n+2)(1+R/\rho)\int_{v_1}^{v_0}\left(\frac{\tan v}{\tan v_0} \times \left(A+B\frac{\cos^2 v_0}{\cos^2 v}\right)\right)^n \sin v\cdot\cos v\cdot dv\right]^{1/n} \quad (14)$$

where

$$v_1 = \arcsin\left(\frac{R-\delta}{R}\sin v_0\right)$$

3.2 An approximation method of using a stress gradient

Fig. 8 shows how the stress distribution function $f(r)$ and its 10th power vary with r for the case of a Neuber notch of $R/\rho = 7.5$. The latter function decreases very rapidly with r and is nearly zero except within a very thin layer beneath the surface. Therefore, it is supposed that the stress near the notch bottom is dominant for the determination of the fatigue notch factor; in other words, the fatigue notch factor is, as well known, quite determinable from the stress distribution only near the notch bottom. Thus we can avoid the cumbersome calculation of Eq. (14) by approximating the distribution of stresses Eq. (8) by a linear distribution,

$$\sigma = \begin{cases} \sigma_a \alpha\chi(r+1/\chi-R)\cdot\cos w & (R-1/\chi \leqq r \leqq R) \\ 0 & (0 \leqq r \leqq R-1/\chi) \end{cases} \quad (15)$$

where

$$\chi = \frac{1}{\sigma_p}\left.\frac{d\sigma}{dr}\right|_{r=R}$$

with

$$\sigma_p = \sigma|_{r=R} \qquad \alpha = \sigma_p / \sigma_a$$

In this approximation, the heat generation rate is

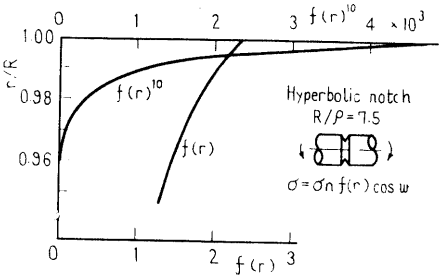

Fig. 8 Variations of stress distribution function $f(r)$ and its 10th power $f^{10}(r)$ for a deep hyperbolic notch of R/ρ=7.5

$$H_{\text{notched}} = C_4\int_{R-S}^{R}\left(\frac{\sigma_w}{\beta}\alpha\chi(r+\frac{1}{\chi}-R)\right)^n r dr \quad (16)$$

We have to take the smaller value between δ and $1/\chi$ as S. The fatigue notch factor becomes

$$\beta = \alpha K\left[\frac{n+2}{n+1}\frac{1}{R\chi}\left(1-\frac{1}{n+2}\frac{1}{R\chi}\right)-(1-\chi S)^{n+1} \times\left(\frac{n+2}{n+1}\frac{1}{R\chi}\left(1-\frac{1}{n+2}\frac{1}{R\chi}\right)-\frac{1}{R\chi}\frac{S}{R}\right)\right]^{1/n} \quad (17)$$

Practically, however, the second term can be eliminated, which either exactly vanishes for $S = 1/\chi$ or is negligible compared with the first for $S = \delta$. Thus simply

$$\beta = \alpha K\left[\frac{n+2}{n+1}\frac{1}{R\chi}\left(1-\frac{1}{n+2}\frac{1}{R\chi}\right)\right]^{1/n} \quad (18)$$

Some mention is made of the discrepancy of the values calculated from Eq. (14) and Eq. (18) for a deep hyperbolic notch. For it the stress gradient is

$$\chi = \frac{1}{R}\left[1 + \frac{(A+3B)R}{(A+B)\rho}\right] \quad (19)$$

from Eq. (13). Fig. 9 illustrates the integrands for the exact (a) as well as for

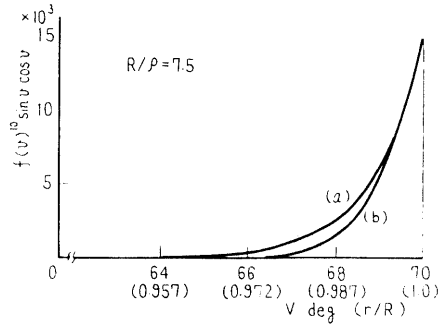

Fig. 9 Comparison of integrands based on exact stress analysis (a) and approximated by use of stress gradient (b)

the approximate (b) calculations. It is seen in Fig. 10 that the calculation by means of the stress gradient gives a little smaller values than by the exact stress distribution; the difference is not so wide, however. For $R/\rho = 7.5$, i.e., $R\chi = 15.95$ as an example, the exact one is $\beta = \alpha/1.31$ and the other $\beta = \alpha/1.28$. The error is only 2~3 %.

An empirical formula given by Siebl et al.[11]

$$\alpha/\beta = 1 + c\sqrt{\chi} \qquad (20)$$

is illustrated in Fig. 10 together with our calculated values. Both agree satisfactorily.

3.3 About the value of K

The factor K in Eq. (10) has turned out to represent the proportion of the part suffering from fatigue damage to the whole sectional area. The authors themselves have nothing to say about the appropriate value of δ. Only they can say that the variation of the K values with δ is rather small for the rotating bending fatigue as known from the numerical values given in Table 2.

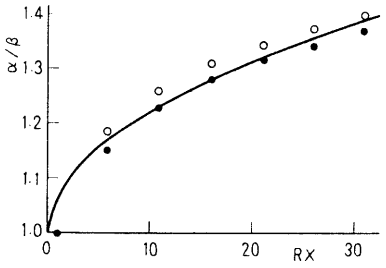

Fig. 10 Difference between notch factors obtained from rigorous stress distribution (solid circles) and from stress gradient (open circles)

3.4 Comparison of the calculted fatigue notch factors with the measured ones

Assuming $\delta = 0.2$ mm and referring to the notch shapes of Nishitani et al.[12][13], the authors have calculated the fatigue notch factors and compared the results with their measurements. The value of the exponent $n = 10$ has been assumed for other steel S20C too, for which it has not been determined yet. Tables 3 and 4 together with Fig. 11 show the results. Close agreement is obtained for various geometries of the notches. It should be noted that the notch factors calculated above are for the fatigue strength because of the characteristics of the above criterion laid down.

4. Discussion

Although the heat generation rate, in this investigation, has been found not to vary with the number of stress cycles, several substages were noticed by Minamizawa et al.[14] in the temperature increase during the main process of the fatigue in their steel specimens of S28C and S30C under reversed plain bending. However, each of the deviations at the transition of those substages is seen rather small. Occurrence of such substages seems to have no effect on the present conclusions any way.

It is known that rapid changes in hardness[15][16] and in energy dissipation[3] occur in what is called the stage I, and also is known that the less the

Table 2 Values of K

R mm \ δ mm	0.1	0.2	0.3	R
5.0	1.17	1.10	1.07	1.00
2.5	1.10	1.05	1.03	1.00

Table 3 Notch factors for S50C, rotating bending

Radius of specimen R mm	Form of notch: depth t mm	Form of notch: root radius ρ mm	Stress gradient χ mm^{-1}	Stress concentration factor α	Measured: fatigue strength σ_w kg/mm^2	Measured: notch factor β	Calculated: Rχ	Calculated: notch factor β
		2.0	1.4	1.43	20.0	1.35	7.0	1.31
		1.0	2.4	1.67	17.5	1.54	12.0	1.45
5.0	0.2	0.6	4.6	1.90	16.5	1.64	23.0	1.54
		0.3	8.0	2.33	15.0	1.80	40.0	1.79
		0.1	22.0	3.39	12.5	2.16	110.0	2.36
		0.3	8.4	1.90	19.0	1.48	21.0	1.48
2.5	0.1	0.1	23.4	2.66	15.0	1.87	58.75	1.87
		0.05	44.1	3.39	12.0	2.34	102.75	2.25

Ref. (12)

Table 4 Notch factors for S20C, rotating bending

Radius of specimen R mm	Form of notch: depth t mm	Form of notch: root radius ρ mm	Stress gradient χ mm^{-1}	Stress concentration factor α	Measured: fatigue strength σ_w kg/mm^2	Measured: notch factor β	Calculated: Rχ	Calculated: notch factor β
5.0	0.2	1.0	2.6	1.67	15.0	1.44	13.0	1.42
		0.6	4.2	1.90	14.0	1.54	21.0	1.55
		0.3	8.0	2.33	12.5	1.72	40.0	1.79
		0.1	22.6	3.39	9.5	2.27	113.0	2.34
2.5	0.1	1.0	2.9	1.43	17.0	1.32	7.25	1.24
		0.6	4.5	1.59	16.0	1.41	11.25	1.32
		0.3	8.4	1.90	15.0	1.50	21.0	1.48
		0.1	23.4	2.66	12.0	1.88	58.5	1.87
		0.05	44.1	3.39	10.0	2.25	110.25	2.24
	0.5	1.0	2.6	1.54	16.0	1.41	6.5	1.35
		0.3	7.6	2.26	12.0	1.88	19.0	1.78
		0.1	21.8	3.46	9.5	2.37	54.5	2.45
	0.05	1.0	3.0	1.35	18.0	1.28	7.5	1.17
		0.3	8.7	1.71	15.5	1.49	21.75	1.33
		0.1	24.3	2.28	13.5	1.70	60.75	1.60
	0.02	1.0	3.1	1.25	20.0	1.15	7.62	1.08
		0.3	9.1	1.49	19.0	1.21	22.75	1.15
		0.1	25.5	1.86	17.5	1.31	63.8	1.30
	0.01	1.0	3.2	1.19	21.0	1.10	8.0	1.02
		0.3	9.4	1.35	20.0	1.15	23.5	1.04
		0.1	26.4	1.62	19.5	1.18	66.0	1.13
							Ref.	(13)

number of slip systems of crystals is, the longer the period is[3]. It is probable that the period is so short for our material that no particular change is recognized in the heat generation rate and consequently no alteration is made of our criterion.

The coefficient σ* in Eq. (5) is "the characteristic drag stress" according to Gilman[8] and represents the resistivity against the movements of dislocation lines. The value may depend on the kinds of materials, on the conditions of heat treatment, and others. Subsequently, the same is true of the exponent n, which is expressible with $1 + \sigma^*/\sigma_w$.

The fatigue criterion Eq. (4) is rewritten, by use of Eq. (6), as

$$(\sigma_a^n - \sigma_w^n) N_f = \text{const.}, \qquad (21)$$

or approximately

$$\sigma_a^n \cdot N_f = \text{const.}, \qquad (22)$$

for fairly larger stress amplitudes than the stress of the fatigue limit, which yields a way to get the value of n from the inclination of the graph of the logarithms of the stress amplitudes and fatigue lives

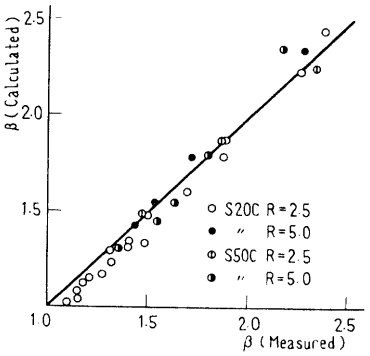

Fig. 11 Comparison between fatigue notch factors calculated and measured

in the region of $\sigma_a \gg \sigma_w$.

The expressions similar to Eq. (22) were already given by several researchers who interpreted the fatigue phenomenon in terms of the hysteresis energy loss, while Eq. (21) is the same expression as Enomoto's (17). Lazan[18] collectively gave $n = 8$ for various materials subjected to larger stresses than their fatigue limits, which value was the average of the values ranging

from 6 to 10 or a little more. Kikukawa et al.[19] gave about 9 to 11 for their steel specimens of S40C and S20C as rolled to crack or to break. It would be said that these values are well compared with our value of n = 10 for S50C.

On the other hand, Morrow[20] gave a summary of 190 sets of data compiled by Halford together with his own and showed that the total plastic strain energy to fracture is not constant but increases with the fatigue life. Such tendency is expected from Eq. (21) when it is written as

$$\sigma_a^n \cdot N_f = \text{const.} + \sigma_w^n \cdot N_f$$

5. Conclusions

The main results of this investigation are briefly summarized as follows:

1) The temperature variation of the specimen due to the fatigue heat generation can be given by an expression involving two exponential functions with due consideration for heat transmission.

2) The heat generation rate, or the generated thermal energy during one stress cycle, seems to be almost constant throughout the main fatigue process and constitutes a fatigue criterion with the fatigue life such as Eq. (4).

3) The heat generation rate depends on the amplitude of the reversed stress and can be expressed by Eq. (5), which envolves a factor so depending on the stress as the mean dislocation velocity does.

4) The formula for calculation of the fatigue notch factor for the fatigue strength is deduced by applying the above fatigue criterion to the notched specimens.

Acknowledgements

The materials used in this experiment were kindly given by Professor H. Nishitani, Institute of Strength of Materials, Faculty of Engineering, Kyushu University. The members of the Institute helped with the heat treatment and electropolishing of the specimens. The authors highly appreciate their courtesy and co-operation.

References

(1) Ono,A., ZAMM,Vol.16, No. 1, (1936), p.23.
(2) Nakamura,H., Tetsudo Gyomu Kenkyu Shiryo (in Japanese), Vol.13, No.1, (1956), p.1.
(3) Wadsworth,N.J., Dislocations and Mechanical Properties of Crystals (ed. J.C.Fisher et al.), Chapt.V, (1957), p.479, John Wiley & Sons.
(4) Higuchi,M., Ishii,H., Imai,Y., Rep. Res. Inst. Appl. Mech., Kyushu Univ., Vol.16, No.55, (1968), p.361.
(5) Higuchi,M., Imai,Y., J. Appl. Polym. Sci., Vol.14, (1970), p.2377.
(6) Imai,Y., Higuchi,M., Proc. Int. Conf. Mech. Beh. Mat., Vol.3, (1972), p.590, JSMS.
(7) Tompson,N., Wadsworth,N.J., Advances in Physics, Vol.7, No.25, (1958), p.72.
(8) Gilman,J.J., J. Appl. Phy., Vol.36, No.10, (1965), p.3195.
(9) Ishibashi,T., Kinzoku no Hiro to Hakai no Boshi (in Japanese), Chapt.IV, (1967), Yokendo.
(10) Neuber,H., Kerbsppannungslehre, (1937), p.81, Springer.
(11) Siebel.E., Stieler,M., Z-VDI, Vol.97, No.5, (1955), p.121.
(12) Nishitani,H., Nishida,S., J. Japan Soc. Strength and Fracture (in Japanese), Vol.5, No.3, (1970), p.84.
(13) Nishitani,H., Preprint of JSME (in Japanese), No.198, (1969), p.37., Trans. JSME (in Japanese), Vol.34, No.259, (1968), p.371.
(14) Minamizawa,C., Aoki,N., Sasabe,T., J. Mat. Sci. Soc. Japan (in Japanese), Vol.8, Nos.4,5, (1971), p.246.
(15) Davies,R.B., Mann,J.Y., Kemsley,D.S., Proc. Int. Conf. Fatigue of Metals, IME, ASME, (1956), p.551.
(16) Wood,W.A., J. Inst. Metals, Vol.91, No.7, (1962-63), p.225.
(17) Enomoto,N., Proc. ASTM., Vol.55, (1955), p.903.
(18) Lazan,B.J., Mechanical Behavior of Materials at Elevated Temperatures, (ed. J.E.dorn), (1961), p.477, McGraw-Hill.
(19) Kikukawa,M., Ohje,K., Johno,M., Mizoguchi,T., Trans. of JSME (in Japanese), Vol.35, No.278, (1969), p.2020, J. of JSME (in Japanese), Vol.70, No. 585, (1967), p.1495.
(20) Morrow,J.D., ASTM STP No.378, (1965).